Journal of Applied Physics

Variable-range-hopping conductivity in high-k $Ba(Fe_{0.5}Nb_{0.5})O_3$ ceramics

Cite as: J. Appl. Phys. **114**, 104106 (2013); https://doi.org/10.1063/1.4821042
Submitted: 16 May 2013 . Accepted: 27 August 2013 . Published Online: 12 September 2013

Shanming Ke, Peng Lin, Huiqing Fan, Haitao Huang, and Xierong Zeng

Variable-range-hopping conductivity in high-k $Ba(Fe_{0.5}Nb_{0.5})O_3$ ceramics

Shanming Ke,[1,2,a)] Peng Lin,[1,2] Huiqing Fan,[3] Haitao Huang,[4,a)] and Xierong Zeng[1,2]
[1]*College of Materials Science and Engineering, Shenzhen University, Shenzhen 518060, China*
[2]*Shenzhen Key Laboratory of Special Functional Materials, Shenzhen 518060, China*
[3]*State Key Laboratory of Solidification Processing, School of Materials Science and Engineering, Northwestern Polytechnical University, Xi'an 710072, China*
[4]*Department of Applied Physics and Materials Research Center, The Hong Kong Polytechnic University, Hung Hom, Kowloon, Hong Kong, China*

(Received 16 May 2013; accepted 27 August 2013; published online 12 September 2013)

The dielectric and transport properties of $Ba(Fe_{0.5}Nb_{0.5})O_3$ ceramics have been investigated in a temperature range of 140–300 K and a frequency range of 1 Hz–10 MHz. The temperature dependence of bulk dc conductivity does not feature an Arrhenius behavior, but indicates a variable-range-hopping mechanism. The observed low temperature relaxation can be perfectly described by a polaronic model, which indicates that the dielectric relaxation is intimately related to the hopping motion caused by localized charge carriers. © *2013 AIP Publishing LLC*. [http://dx.doi.org/10.1063/1.4821042]

I. INTRODUCTION

In the past few years, single phase compounds with perovskite structure, such as lead iron niobate ($Pb(Fe_{0.5}Nb_{0.5})O_3$, PFN), in which electric and magnetic orders coexist, have been widely investigated.[1–3] PFN undergoes a paraelectric-to-ferroelectric phase transition near 373 K and a paramagnetic-to-antiferromagnetic phase transition at the Neel temperature (~143 K). Recently, a similar system, barium iron niobate ($Ba(Fe_{0.5}Nb_{0.5})O_3$, BFN), has attracted much attention because of its giant dielectric response, magnetic properties, and unique dielectric relaxation behaviors.[4–13]

BFN was first studied as a dielectric ceramic by Yokosuka in as early as 1994.[4] It is a spin-glass showing weak ferromagnetic behavior below 25 K,[5,6] and it was reported as a lead-free ferroelectric relaxor in 2002.[7,8] Raevski and Chen *et al.*[9,10] argued later that BFN is not a ferroelectric and the high temperature relaxor-like dielectric peaks were attributed to oxygen vacancy induced dielectric abnormity. Recently, first-principle computations verified that BFN is really not a ferroelectric material.[11] In addition to this dispute, BFN is fascinating because it has a giant dielectric constant in the order of 10^4, which is almost independent of temperature in a wide range,[4,9,10,12] and is very similar to that of the well-known non-ferroelectric material, $CaCu_3Ti_4O_{12}$ (CCTO).[13,14]

In our previous study, two dielectric relaxations were observed in BFN at both low and high temperatures,[15] and a giant dielectric tunability can be obtained under a low bias field at room temperature.[16] The strong nonlinear current-voltage characteristics of BFN showed a typical behavior of ceramic varistors, which implies highly conducting grain bulk. However, the conduction mechanism in BFN is still far from well understood. In this paper, we present a systematic study on the low temperature transport and dielectric relaxation of BFN ceramics. Our results indicate that, due to the mixed valences of Fe, the Mott's variable-range-hopping (VRH) conduction exists in BFN bulk ceramics at low temperatures. A polaronic relaxation model was proposed as a possible explanation to the low temperature dielectric relaxation.

II. EXPERIMENTAL PROCEDURE

Single phase BFN powders were obtained using "columbite" process with $BaCO_3$ and $FeNbO_4$ (FN) as the precursors. The details can be found in our previous work.[12] BFN pellets were densified by cold isostatic pressing and then sintered at 1250–1350 °C for 6 h. The samples obtained by the "columbite" method were named BFN-C-T_s (T_s refers to the sintering temperature, e.g., BFN-C-1250). Another type of sample was called BFN-M-T_s, which was synthesized by a direct mixed oxide method. In this method, reagent grades Fe_2O_3, $BaCO_3$, and Nb_2O_5 were directly mixed and ball milled. The mixture was dried and calcined and finally sintered in air at 1250–1350 °C.

The crystalline structure and phase purity were confirmed by X-ray diffraction (XRD, Philips, X'Pert-Pro MPD) and Micro-Raman spectroscopy (JY HR800, 15 mW argon ion laser at 488 nm was used as the excitation source). X-ray photoelectron spectroscopy (XPS, Physical Electronics, PHI-5600) was also performed on the polished BFN surfaces at room temperature. Silver paint was coated on both surfaces of the sintered disks and fired at 650 °C for 20 min. The dielectric properties were measured by using a frequency-response analyzer (Novocontrol Alpha-analyzer) over a broad frequency range (1 Hz–10 MHz) at various temperatures down to 140 K.

III. RESULTS AND DISCUSSION

A. Local symmetry of BFN

Since the early 1960s, BFN has been known as a cubic perovskite with the lattice parameter $a = 0.8118$ nm.[17] However, experimental Raman spectra reveal a lower

a)Authors to whom correspondence should be addressed. Electronic addresses: keshanming@gmail.com and aphhuang@polyu.edu.hk

symmetry than cubic in local regions. Fig. 1(a) shows the reduced Raman spectra of BFN-C-1300 and BFN-M-1300 at room temperature, in which the population factor $n(\nu+1)$ is considered.[18] The lowest-wave number peak around 113 cm^{-1} could be assigned as F_{2g} mode,[19] which is predominantly caused by the motion of Ba^{2+} ions against the oxygen octahedron in 1:1 ordered or related compounds. By using Lorentzian fitting, notable splitting of this vibration mode into two Raman peaks could be observed, which implies the lowering of local symmetry from cubic.

Another characteristic feature in Raman spectrum of BFN is the two-mode-like behavior of A_{1g} mode observed in the range of 650–850 cm^{-1}. Similar behavior has been reported in $Pb(Mg_{1/3}Nb_{2/3})O_3$-$PbTiO_3$ (Ref. 20) and $BaCe_xZr_{1-x}O_3$ (Ref. 21) complex perovskite systems. Generally, the two-mode-like behavior could be regarded as a consequence of local phase-segregation or compositional fluctuation.[20,21] For BFN, it is most probably that Fe rich and Nb rich regions coexist. The Lorentzian fitting results of these two bands are shown in Figs. 1(b)–1(d) within three main Lorentzian peaks, which clearly indicate that the compositional fluctuation of BFN is strongly processing dependent. Accordingly, the peak 3 at around 780 cm^{-1} could be assigned to the motion of NbO_6 octahedron, while the peak 2 at around 715 cm^{-1} could be caused by FeO_6 octahedron. It is suggested that the peak 1 centered at the lowest wave number below 700 cm^{-1} could be probably due to the octahedral distortion in the fluctuation region. The BFN-M sample shows much higher intensity and larger full width at half maximum (FWHM) of peak 1 than BFN-C, which implies that direct mixed oxide method cause stronger compositional fluctuation. In addition, our previous XRD data have confirmed the cubic $Fm\bar{3}m$ symmetry for all samples.[15] So, the compositional fluctuation or the deviation from cubic symmetry should be considerably weak.

B. VRH conduction

Fig. 2(a) shows the frequency dependence of the conductivity σ' at various temperatures for BFN-C-1300 (the result of the other samples is similar). Similar to an earlier report in CCTO,[22] there is a rapid increase at low frequencies and a slow increase at high frequencies. Up to now, there is no unambiguous explanation to ascribe the strong rise at low frequencies to the grain-boundary blocking effect[22] and the left wing of the dielectric peak to the hopping relaxation.[23] The σ' in the high frequency range, which is the bulk conductivity relaxation in which we are primarily interested, can be described by the "universal dielectric response" (UDR)[24]

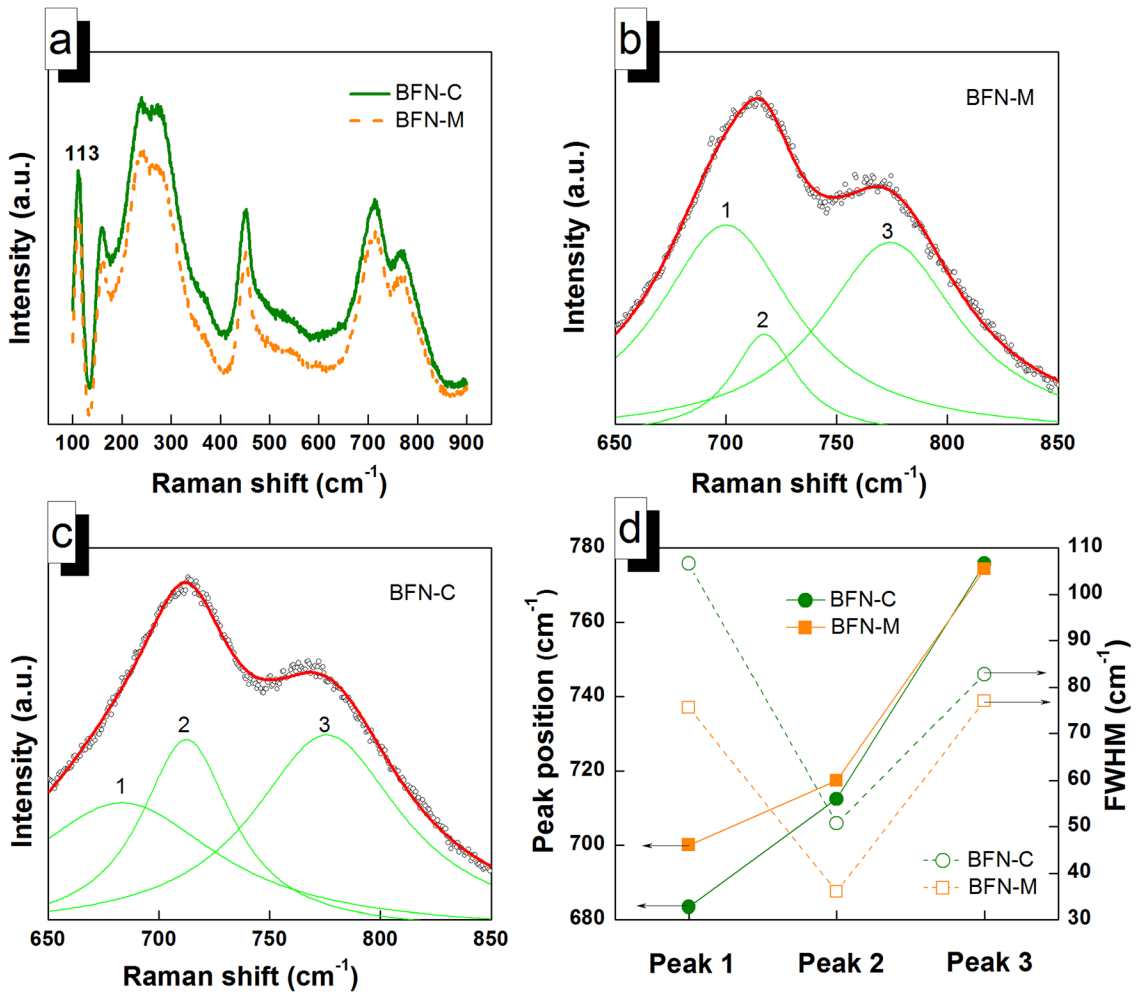

FIG. 1. (a) Reduced Raman spectra of BFN-C-1300 and BFN-M-1300 ceramics; (b) and (c) experimental data (dots) and fitted Lorentzian curves (solid lines) for BFN-M-1300 and BFN-C-1300, respectively; (d) summary of the fitting results.

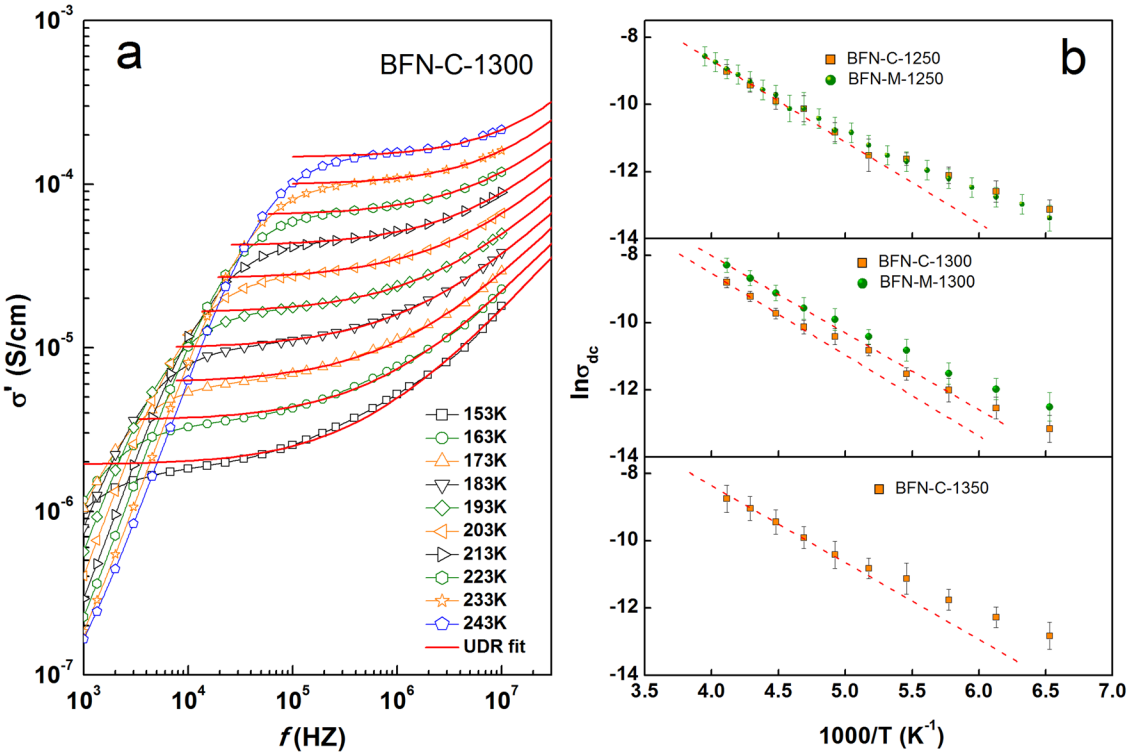

FIG. 2. (a) Frequency dependence of conductivity σ' at selected temperatures for BFN-C-1300. The solid lines are fitted according to Eq. (1); (b) the Arrhenius relations between the σ_{dc} and the temperatures T obtained from Eq. (1) for BFN ceramics.

$$\sigma'(f) = \sigma_{dc} + \sigma_0 f^s, \tag{1}$$

where f is the experimental frequency, σ_{dc} is the "dc bulk conductivity" and $0 < s < 1$. Equation (1) is typical for thermally assisted tunneling between localized states. In CCTO, it has been attributed to the polaron relaxation related to the localized charge carriers.[22,25] The solid lines in Fig. 2(a) are the best fit to Eq. (1).

In the hopping conduction of charge carriers, the nearest-neighbor hopping obeys the Arrhenius law and the VRH obeys the Mott's VRH equation[26]

$$\sigma_{dc} = \sigma_1 \exp[-(T_0/T)^{1/\gamma}], \tag{2}$$

where σ_1 is constant, $\gamma = 2$, 3, or 4, depending on the conduction mechanism. T_0 is the parameter related to the density of localized states at the Fermi level and the decay length of the localized wave function. From Fig. 2(b), it could be found that the obtained σ_{dc} for all samples does not follow the Arrhenius law over a significant temperature range, and therefore the nearest-neighbor hopping mechanism can be excluded.

Fig. 3 shows the dc conductivity versus the inverse quarter power of temperature. The solid line is the best fitted curve of the experimental data according to Eq. (2) with the exponent $\gamma = 4$. It can be seen that the inverse quarter power law predicted by the VRH mechanism describes the bulk conductivity of BFN perfectly well, as that in CCTO.[22] From Mott's VRH model,[26] we also could obtain the hopping energy

$$W = 0.25 k_B T_0^{1/4} T^{3/4}. \tag{3}$$

The temperature dependence of the W values is plotted in Fig. 3(a). For all samples, the hopping energy W increases monotonically in the range of 0.12–0.20 eV at temperatures from 150 to 260 K.

The exponent parameters $s(T)$ obtained from Eq. (2) are shown in Fig. 4 for selected BFN samples. A minimum at about 183 K in $s(T)$ shows up for both samples. Such a minimum in $s(T)$ is predicted by the "overlapping large-polaron tunneling" (OLPT) model.[27] In the OLPT model, the charge carriers are assumed to be large polarons, i.e., the lattice distortion around the site of a charge carrier overlaps with the distortions on neighboring sites. This gives rise to an energy barrier which is a function of the site separation. According to the OLPT model suggested by Long *et al.*, the expressions for ac conductivity and exponent s are described as[27]

$$\sigma'(\omega) = \sigma_{dc} + \frac{\pi^4 e^2 k_B^2 [N(E_f)]^2}{12} \times \frac{\omega R_\omega^4}{2\alpha k_B T + (W_{HO} r_p)/R_\omega^2}, \tag{4}$$

$$\mathrm{s(T)} = 1 - \frac{4 + 6W_{HO} r_p'/k_B T R'^2_\omega}{\left(1 + \frac{W_{HO} r_p'}{k_B T R'^2_\omega}\right)^2} \times \frac{1}{R'_\omega}, \tag{5}$$

where $r_p' = 2\alpha\gamma_p$ (r_p is the polaron radius and α is the wave function decay constant), $R'_\omega = 2\alpha R_\omega$ (R_ω is the optimum hopping length), W_{HO} is activation energy associated with charge transfer between the overlapping sites. For small values of r_p, $s(T)$ exhibits a minimum at a certain temperature around $0.1W_{HO}/k_B$ and subsequently increases with increasing temperature, similar to the case of small-polaron tunneling (SPT) model.[27]

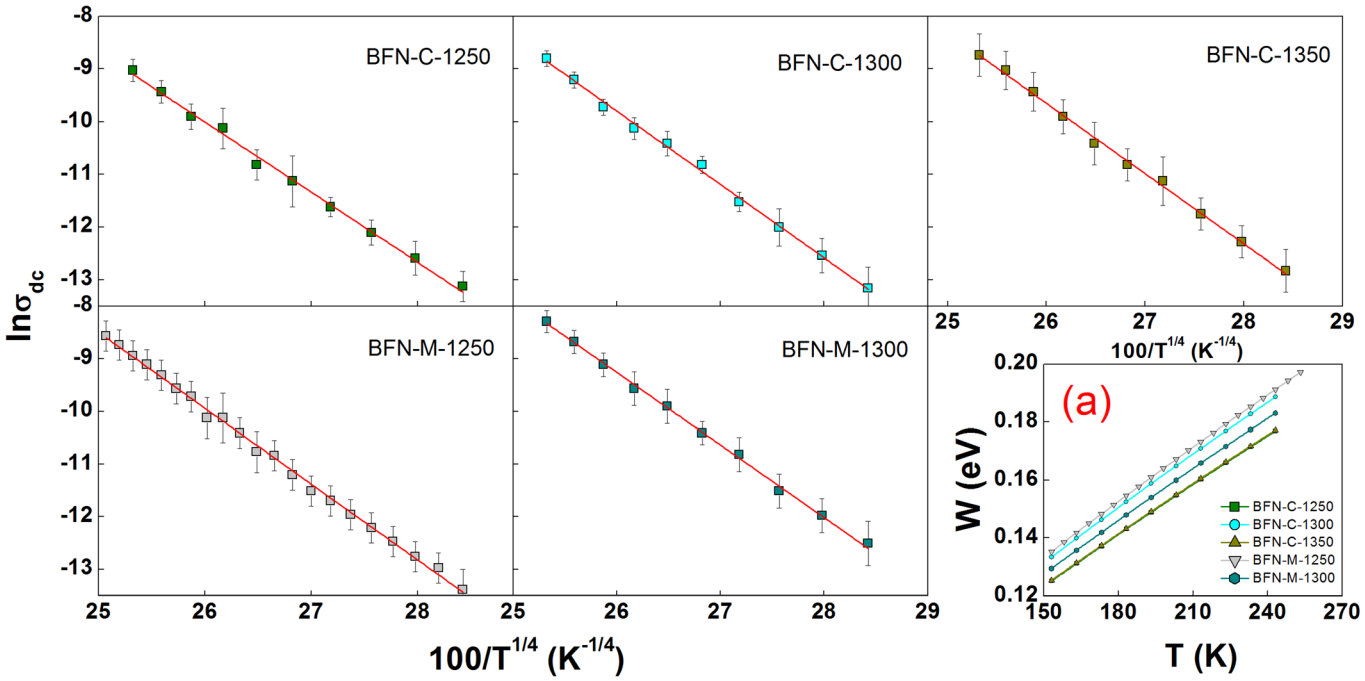

FIG. 3. Temperature dependent bulk dc conductivity σ_{dc} for BFN ceramics scaled for thermally activated Variable-range-hopping of charges and (a) hopping energies W.

The experimental data of ac conductivity have been fitted with Eq. (4) for all the studied samples and a typical fitting for BFN-C-1300 is shown in Fig. 5. It is noted that OLPT model gives very good agreement at high temperatures. But at lower temperatures, it shows deviations in intermediate frequency region. The reason for this deviation may be due to the ignoring of either the frequency dependence of R_ω during fitting or the change of local structure of the ceramics with temperature. The parameters obtained from fitting of experimental data of ac conductivity with Eq. (4) are listed in Table I and the W_{HO} values agree well with those obtained from fitting of dc conductivity data with VRH model. For a OLPT process,[28] the exponent s_{min} is also expressed to be $s_{min} = 1–5/2(W_{HO}\gamma_p'/kT)^{1/2}$. The resulting energy barrier for infinite distance of the polaron sites is $W_{HO} = 0.16$ eV, which is comparable to the values listed in Table I and to that for OLPT conduction in $La_{0.95}Sr_{0.05}MnO_3$ (0.2 eV).[29]

C. Discussion

The Raman spectrum of BFN reveals a lower symmetry than cubic in local regions (see Fig. 1). Shuvaeva *et al.*[30] have reported that the low local symmetry is inherent to most of ternary Nb-containing perovskites, as confirmed by the extended x-ray absorption fine structure (EXAFS) study. In these compounds, Nb occupies an off-center position,

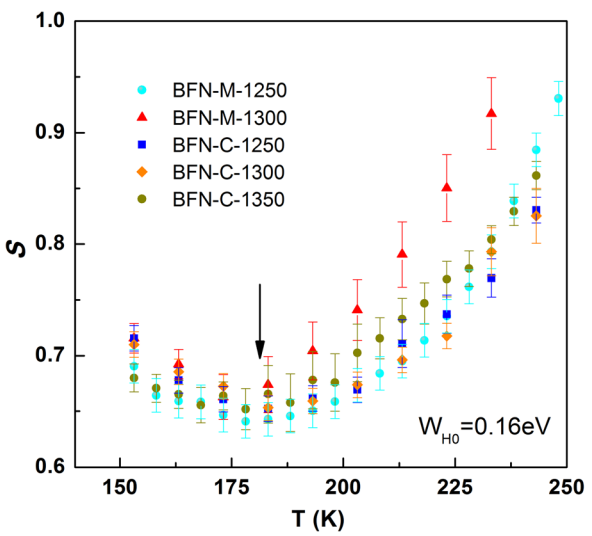

FIG. 4. Temperature dependence of the exponent $s(T)$ obtained from the fitting according to Eq. (1).

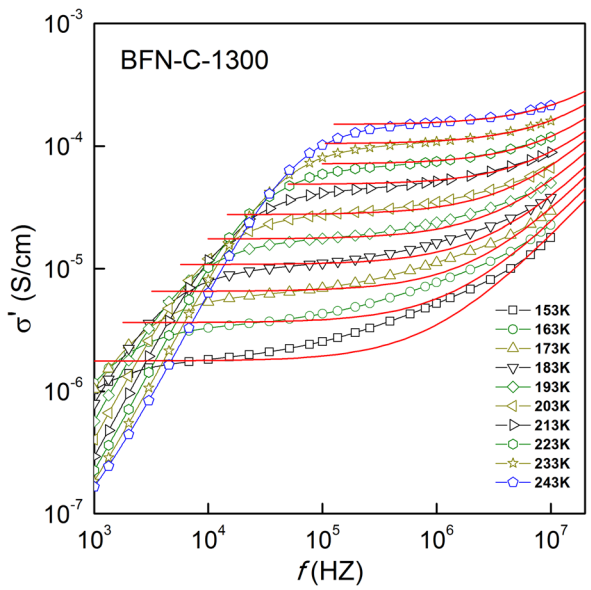

FIG. 5. (a) Frequency dependence of conductivity σ' at selected temperatures for BFN-C-1300. The solid lines are fitted according to Eq. (4).

TABLE I. Parameters obtained from the fitting of experimental data of ac conductivity with OLPT model for BFN ceramics.

Parameters	BFN-C-1250	BFN-C-1300	BFN-C-1350	BFN-M-1250	BFN-M-1300
r_p (nm)	0.69	0.83	0.92	0.86	0.97
α (nm^{-1})	0.089	0.093	0.091	0.091	0.095
W_{HO} (eV)	0.15	0.16	0.16	0.18	0.19

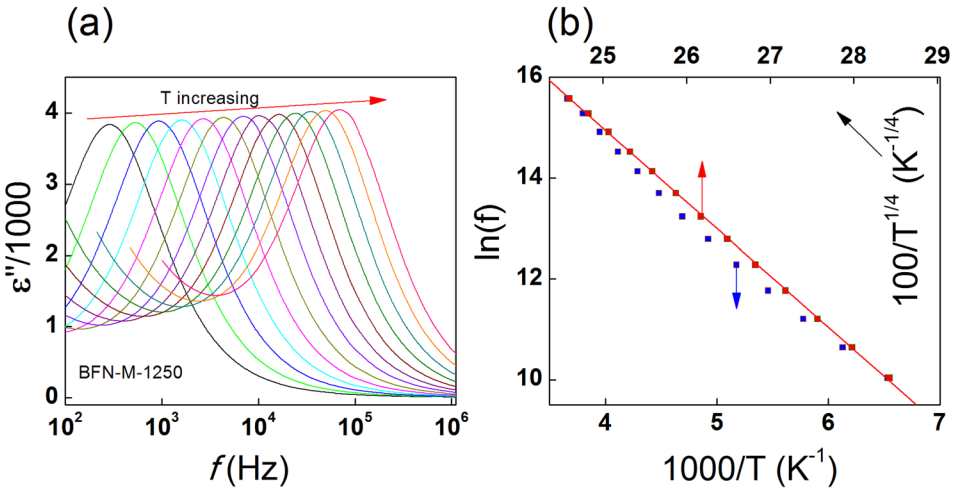

FIG. 6. (a) Frequency dependence of dielectric loss ε'' at selected temperatures for BFN-M-1250; (b) the Arrhenius and VRH-like plots for the relaxation frequencies. The solid line is a fitting curve according to Eq. (6).

leading to a lower symmetry accordingly.[30] From this point of view, the low local symmetry in BFN is quite expectable.

We assumed the two-mode-like behavior (see Fig. 1) in Raman spectrum of BFN was due to the existence of Fe rich as well as Nb rich regions according to the peak fitting. Clues may be found in a similar 1:1 composition, PFN. Fe and Nb were generally deemed to distribute randomly in PFN lattice. However, Fe rich with Nb poor and Fe poor with Nb rich regions have been confirmed recently in PFN by the ^{93}Nb NMR spectra and ^{57}Fe Mössbauer spectra.[31,32] On the basis of first-principles calculations, Raevski *et al.*[32] pointed out that the probability of Fe clustering in BFN is much lower than that in PFN. It is then assumed that peak 1 in Fig. 1 is most probably caused by the compositional fluctuation of Nb clustering in BFN.

The ac bulk conductivity of BFN shows a power-law behavior and the dc bulk conductivity is found to obey Mott's VRH mechanism. It is then suggested that the transport behavior in the bulk ceramics indicates clearly a large polaron relaxation. From Fig. 3(b), it could be found that the conductivity is strongly dependent on the sintering temperature, which is probably due to partial reduction of iron valence state from Fe^{3+} to Fe^{2+} at high temperatures.[33] The Fe^{2+} and Fe^{3+} can form Fe^{2+}-O-Fe^{3+} bonds and the Fe-3*d* electrons in Fe^{2+} ions can hop to Fe^{3+} under an applied field. The formation of larger Fe^{2+} ions (ionic radius $Fe^{2+} = 0.074$ nm, $Fe^{3+} = 0.064$ nm) will distort the lattice and produce a polaronic distortion. The valence state of Fe ions in Fe-containing compounds is usually determined by XPS technique. It is well known that, due to the spin-orbit coupling, the Fe 2p core level is split into the $2p_{1/2}$ and $2p_{3/2}$ components. For Fe^{2+} iron, the $2p_{3/2}$ core level appears at 709.4–710 eV while for Fe^{3+} ion it appears at 710.8–711 eV.[34] However, deconvolution of the Fe $2p_{3/2}$ peak into two peaks according to the Fe^{2+} and Fe^{3+} states seems highly speculative. Recently, the problem of XPS approach to the estimation of Fe^{2+}/Fe^{3+} ratio has been discussed thoroughly by Kozakov *et al.*[35] They confirmed that the presence of Fe^{2+} is manifested by a small shoulder on the Fe $2p_{3/2}$ peak. Such feature

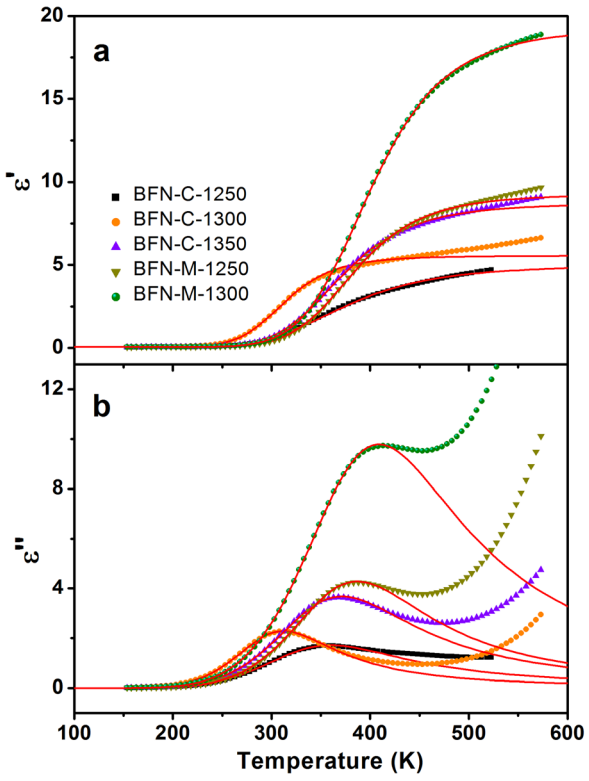

FIG. 7. Temperature dependent dielectric permittivity ε' at 1 MHz for BFN ceramics, the solid lines are fitting curves according to Eqs. (8) and (9).

TABLE II. Parameters obtained from the fitting of experimental data of dielectric permittivity at 1 MHz with Eqs. (8) and (9) for BFN ceramics.

Parameters	BFN-C-1250	BFN-C-1300	BFN-C-1350	BFN-M-1250	BFN-M-1300
A	0.98888	0.98746	0.99359	0.99984	0.99987
ε_0	56	56	56	56	56
γ_0 (Hz)	3.18×10^{10}	9.72×10^{10}	1.77×10^{11}	2.81×10^{11}	4.45×10^{11}
E (eV)	0.150	0.171	0.169	0.188	0.186

is not seen in XPS spectrum of our BFN samples (not shown). Mössbauer spectra[6,33] also indicate that only Fe^{3+} exists in BFN ceramics. Since we have no clearly evidence on the existence of Fe^{2+} ions, it is doubtful that the coexistence of Fe^{2+} and Fe^{3+} ions is the main microscopic origin of the polaron behaviors. Other sources, such as the compositional fluctuation with localized charge carriers (see Sec. III A) can also produce distortion and contribute to the microscopic origin of polaron behaviors. It should be emphasized that the origin of the polaron behavior and corresponding Mott's VRH conduction in BFN is still obscure and needs further studies.

From the relationship between the conductivity and the dielectric permittivity, $\varepsilon''(\omega) = \sigma'(\omega)/\omega$, it is reasonable to predict that the large polaron hopping process will also affect the dielectric permittivity. Fig. 6(a) illustrates the frequency dependence of ε'' at temperatures varying from 153 to 273 K with 10 K increment for BFN-M-1250. It is found that the peak intensity increases gradually as the peak shifts to higher frequencies. Besides, the peak frequency *cannot* be well fitted by the Arrhenius law but by a VRH-like relation suggested by Zhang and Tang[22] [as shown in Fig. 6(b)]

$$f_r = f_0 \exp[(T_0/T_p)^{1/4}], \tag{6}$$

where T_0 is a constant related to the activation energy. This result implies an intimate relationship between the observed dielectric permittivity and the conductivity produced by polaron hopping transport. It leads to a conclusion that the dielectric relaxation frequency f_r is directly related to the dc bulk conductivity.

Taking into consideration the relaxation of polarons occurring at a rate γ determined by the energy barrier between alternate equivalent configurations and the temperature, we get

$$\gamma = \gamma_0 \exp(-E/k_B T), \tag{7}$$

where E is the barrier energy and γ_0 depends on the effective mass of the polarons. As suggested by Ramirez *et al.*,[36] a mean-field approximation can be adopted and the dielectric response can be then calculated as

$$\varepsilon'(\omega, T) = \frac{\varepsilon_0[(1-a)\gamma^2 + \omega^2]}{(1-a)^2\gamma^2 + \omega^2}, \tag{8}$$

$$\varepsilon''(\omega, T) = \frac{\varepsilon_0 a\gamma\omega}{(1-a)^2\gamma^2 + \omega^2}, \tag{9}$$

where ε_0 is the dielectric constant at zero temperature and a is a dimensionless parameter which depends on the polaron concentration and the polarizability of the polaron. We use one representative data set of the ε' at 1 MHz for the least-squares fit of Eqs. (8) and (9). The solid lines in Fig. 7 are the model calculations, which reproduce the experimental data very well. The best result was listed in Table II. It is interesting to note that the obtained barrier energy E is quite close to the activation energy W_{HO} (see Table I) and VRH hopping energy W [see Fig. 3(a)]. Meanwhile, the value of γ_0 is of the order of 10^{10}–10^{11} Hz for all samples, which is fairly reasonable. These results definitely indicate that the studied dielectric relaxation in Fig. 7 is caused mainly by a polaronic relaxation.

IV. CONCLUSIONS

In summary, we have investigated the temperature dependence of ac conductivity and dielectric permittivity spectra of polycrystalline BFN. The ac conductivity of BFN shows a power law behavior at high frequencies and the dc bulk conductivity is found to obey VRH mechanism. The bulk conduction behavior of BFN can be well explained by the OLPT model. The coexistence of Fe^{2+} and Fe^{3+} ions is assumed to be a microscopic origin of the polaron behaviors. However, it is still obscure and needs further studies. The polaron model can also be used to explain the temperature and frequency dependent dielectric permittivity of BFN successfully.

ACKNOWLEDGMENTS

This work was supported by the Hong Kong Polytechnic University (Project Nos. A-PL54 and 1-BD08), the National Natural Science Foundations of China (No. 51302172), the Natural Science Foundation of SZU (Grant No. 00035692), and Shenzhen Innovation and Technology Commission under the strategic emerging industries development project (Contract No. ZDSY20120612094418467).

[1]M. H. Lente, J. D. S. Guerra, G. K. S. de Souza, B. M. Fraygola, C. F. V. Raigoza, D. Garcia, and J. A. Eiras, Phys. Rev. B **78**, 054109 (2008).
[2]V. V. Bhat, A. M. Umarji, V. B. Shenoy, and U. V. Waghmare, Phys. Rev. B **72**, 014104 (2005).
[3]S. P. Singh, A. K. Singh, D. Pandey, H. Sarma, and O. Parkash, J. Mater. Res. **18**, 2677 (2003).
[4]M. Yokosuka, Jpn. J. Appl. Phys., Part 1 **34**, 5338 (1995).
[5]N. Rama, J. B. Philipp, M. Opel, K. Chandrasekaran, V. Sankaranarayanan, R. Gross, and M. S. Ramachandra Rao, J. Appl. Phys. **95**, 7528 (2004).
[6]K. Tezuka, K. Henmi, and Y. Hinatsu, J. Solid State Chem. **154**, 591 (2000).
[7]S. Saha and T. P. Sinha, Phys. Rev. B **65**, 134103 (2002).
[8]S. Saha and T. P. Sinha, J. Phys.: Condens. Matter. **14**, 249 (2002).

[9]I. P. Raevski, S. A. Prosandeev, A. S. Bogatin, M. A. Malitskaya, and L. Jastrabik, J. Appl. Phys. **93**, 4130 (2003).
[10]Z. Wang, X. M. Chen, L. Ni, and X. Q. Liu, Appl. Phys. Lett. **90**, 022904 (2007).
[11]R. Demirbilek, A. I. Gubaev, A. B. Kutsenko, S. E. Kapphan, I. P. Raevski, S. A. Prosandeev, B. Burton, L. Jastrabik, and V. S. Vikhnin, Ferroelectrics **302**, 279 (2004).
[12]S. M. Ke, H. T. Huang, H. Q. Fan, H. L. W. Chan, and L. M. Zhou, Ceram. Int. **34**, 1059 (2008).
[13]S. M. Ke, H. T. Huang, and H. Q. Fan, Appl. Phys. Lett. **89**, 182904 (2006).
[14]D. C. Sinclair, T. B. Adams, F. D. Morrison, and A. R. West, Appl. Phys. Lett. **80**, 2153 (2002).
[15]S. M. Ke, H. Q. Fan, and H. T. Huang, J. Electroceram. **22**, 252 (2009).
[16]S. M. Ke and H. T. Huang, J. Appl. Phys. **108**, 064104 (2010).
[17]I. P. Raevski, S. A. Prosandeev, and I. A. Osipenko, Phys. Status Solidi B **198**, 695 (1996).
[18]R. Loudon, Adv. Phys. **13**, 423 (1964).
[19]W. Zhang, Z. Wang, and X. M. Chen, J. Appl. Phys. **110**, 064113 (2011).
[20]B. Chaabane, J. Kresel, T. Pagnier, G. Lucazeau, and B. Dkhil, Phys. Rev. B **70**, 134114 (2004).
[21]C. Chemarin, N. Rosman, T. Pagnier, and G. Lucazeau, J. Solid State Chem. **149**, 298 (2000).
[22]L. Zhang and Z. J. Tang, Phys. Rev. B **70**, 174306 (2004).
[23]M. Pollak and B. Shklovskifi, *Hopping Transport in Solids* (Elsevier Science Pub. Co., Amsterdam, NY, 1991).
[24]A. K. Jonscher, *Dielectric Relaxation in Solids* (Chelsea, London, 1983).
[25]C. C. Wang and L. W. Zhang, Appl. Phys. Lett. **90**, 142905 (2007).
[26]N. F. Mott and E. A. Davis, *Electronic Processes in Non-crystalline Materials* (Claredon, Oxford, 1979).
[27]S. R. Elliott, Adv. Phys. **36**, 135 (1987); A. R. Long, *ibid*. **31**, 553 (1982).
[28]S. Chakraborty, M. Sadhukhan, D. K. Modak, K. K. Som, H. S. Maiti, and B. K. Chaudhuri, Philos. Mag. B **71**, 1125 (1995).
[29]A. Seeger, P. Lunkenheimer, J. Hemberger, A. A. Mukhin, V. Yu Ivanov, A. M. Balbashov, and A. Loidl, J. Phys.: Condens. Matter **11**, 3273 (1999).
[30]V. A. Shuvaeva, I. Pirog, Y. Azuma, K. Yagi, K. Sakaue, H. Terauchi, I. P. Raevski, K. Zhuchkov, and M. Y. Antipin, J. Phys.: Condens. Matter **15**, 2413 (2003).
[31]V. V. Laguta, J. Rosa, L. Jastrabik, R. Blinc, P. Cevc, B. Zalar, M. Remskar, S. I. Raevskaya, and I. P. Raevski, Mater. Res. Bull. **45**, 1720 (2010).
[32]I. P. Raevski, S. P. Kubrin, S. I. Raevskaya, D. A. Sarychev, S. A. Prosandeev, and M. A. Malitskaya, Phys. Rev. B **85**, 224412 (2012).
[33]I. P. Raevski, S. A. Kuropatkina, S. P. Kubrin, S. I. Raevskaya, V. V. Titov, D. A. Sarychev, M. A. Malitskaya, A. S. Bogatin, and I. N. Zakharchenko, Ferroelectrics **379**, 48 (2009).
[34]N. S. McIntyre and D. G. Zetaruk, Anal. Chem. **49**, 1521 (1977).
[35]A. T. Kozakov, A. G. Kochur, K. A. Googlev, A. V. Nikolsky, I. P. Raevski, V. G. Smotrakov, and V. V. Yeremkin, J. Electron Spectrosc. Relat. Phenom. **184**, 16 (2011).
[36]A. P. Ramirez, G. Lawes, V. Butko, M. A. Subramanian, and C. M. Varma, e-print arXiv:cond-mat/0209498.